

X), and for "magnetic equivalence" cross peak the same intersection coincides with the chemical shift of equivalent nuclei (A_2). In the SECSY spectrum B, we cannot decide connectivities between G3 and G4 and between F3 and F4 due to severe overlap of G3 and F3. However, the circled cross peak shown in DECSY spectrum C indicates that the resonance at about 5 ppm is remote connected with G2 resonance and is thus assigned to G4 proton. The combined use of two DECSY spectra A and C is expedient to facilitate the analysis of complex spectra.

We should emphasize that DECSY is superior to conventional double-quantum coherence spectroscopy with respect to narrower spectral width in the ω_1 dimension and to conventional SECSY with respect to the absence of strong auto peaks. Furthermore, valuable information about remote connectivity and magnetic equivalence can be obtained. These characteristics will take advantage in studying large molecules such as proteins.^{13,14}

In addition, DECSY can be modified to a COSY-type data presentation, which is accomplished by the following pulse sequence: $90^\circ - \tau - 180^\circ - \tau - 90^\circ - t_1 - \alpha - t_1 - \text{acquisition}$. Extension to higher order multiple-quantum coherence echo spectroscopy will be possible using the selective excitation and detection phase cyclings.¹⁰

Acknowledgment. This research is supported by the Ministry of Education, Science, and Culture of Japan. We are indebted to K. Higuchi of JEOL Co. Ltd. for constructing the phase shifter.

(13) Nagayama, K.; Wüthrich, K. *Eur. J. Biochem.* **1981**, *114*, 365.

(14) Arseniev, A. S.; Winder, G.; Joubert, F. J.; Wüthrich, K. *J. Mol. Biol.* **1982**, *159*, 323.

X-ray Crystal Structure of *N*-(2-Lithiocyclohexenyl)-*N,N,N'*-trimethyl-1,3-propanediamine: A Pentavalent Lithium?

Robin L. Polt and Gilbert Stork

*Department of Chemistry, Columbia University
New York, New York 10027*

Gene B. Carpenter and Paul G. Williard*

*Department of Chemistry, Brown University
Providence, Rhode Island 02912*

Received January 26, 1984

Revised Manuscript Received May 18, 1984

Vinyl lithium derivatives are useful tools for the synthesis of organic molecules. Due to a complete lack of structural information about this important class of compounds, we were stimulated to obtain the X-ray crystal structure of the vinyl lithium reagent **1**.¹ This is the first X-ray crystal structure of an organovinyl lithium derivative.^{2,3}

Pure crystalline **1** is easily handled in an inert atmosphere of argon. These crystals are stable over a month in a sealed vial in the presence of solvent (cyclohexane) but undergo a gradual

(1) A series of α -heteroatom substituted β -lithiated vinyl reagents have been prepared by exchange of halogen or Sn with lithium. To date none of these reagents have been isolated as crystalline solids, cf.: (a) Ficini, J.; Falou, S.; Touzin, A.-M.; d'Angelo, J. *Tetrahedron Lett.* **1977**, 3589 (b) Wollenberg, R. H.; Albizzati, K. F.; Peries, R. *J. Am. Chem. Soc.* **1977**, *99*, 7365. (c) Lou, K. S. Y.; Schlosser, M. *J. Org. Chem.* **1978**, *43*, 1595. (d) Kowalski, C. J.; O'Dowd, M. L.; Burke, M. C.; Fields, K. W. *J. Am. Chem. Soc.* **1980**, *102*, 5411. (e) Duhamel, L.; Poirier, J.-M. *Bull. Chem. Soc. Fr.* **1982**, 9-10 (2), 297.

(2) For a comprehensive review of the few crystal structures of aliphatic and aryllithium derivatives, see: Wardell, J. L. in "Comprehensive Organometallic Chemistry"; Wilkinson, G.; Stone, F.G.A., Abel, E. W., Eds.; Pergamon Press: Oxford, 1982; Vol. I, p 65, 84.

(3) Recently, the X-ray crystal structures of two THF-solvated lithium enolates have been described, cf.: Amstutz, R.; Schweizer, W. B.; Seebach, D.; Dunitz, J. D. *Helv. Chem. Acta.* **1981**, *64*, 2617. It is clear that there is no sp^2 C-Li bonding in these solvated enolates.

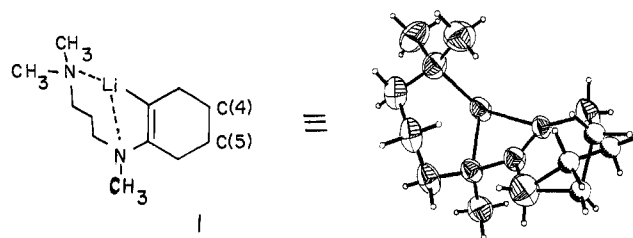


Figure 1.

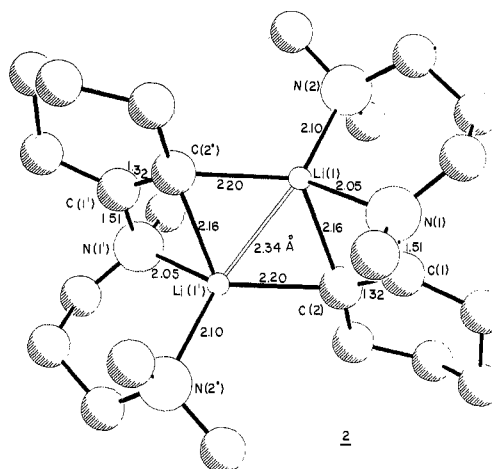


Figure 2. Bond Angles for the Dimer **2**: N(1)-Li(1)-N(2) 103.0, N(1)-Li(1)-C(2) 69.3, N(1)-Li(1)-Li(1') 105.5, N(1)-Li(1)-C(2') 129.2, N(2)-Li(1)-C(2) 114.7, N(2)-Li(1)-Li(1') 144.4, N(2)-Li(1)-C(2') 117.1, C(2)-Li(1)-C(2') 115.0, C(2)-Li(1)-Li(1') 58.3.

decomposition over a period of weeks in the absence of solvent. A single crystal of **1** sealed in a 0.5-mm glass capillary under argon was utilized for x-ray diffraction analysis.⁴

The crystallographic asymmetric unit of **1** is the monomeric species illustrated in Figure 1. The initial refinement of this structure ($R_w = 0.083$)⁵ leads to a planar cyclohexene ring with a shortened σ bond between C(4) and C(5). These two carbon atoms also exhibited elongated thermal parameters in a direction perpendicular to the plane of the cyclohexene ring. This situation is indicative either of a dynamic equilibrium between two half-chair conformations or of an analogous static disorder in the crystal. In either case a more realistic description and better agreement ($R_w = 0.0702$)⁵ was obtained by refinement of a model with four half-methylene groups (site occupation factor = 0.50)⁶ shown together in the computer generated plot of **1** in Figure 1.

The asymmetric units of **1** are sufficiently close to the crystallographic inversion centers so that two of these units form an associated dimer shown in Figure 2 as **2**. Dimeric association allows for coordination of a single lithium atom with four donor ligands (e.g., Li(1) with N(1), N(2), C(2), and C(2')). It is not clear whether this dimer remains associated in solution. Other solution-phase dimeric species have been proposed on the basis of NMR studies for two aryllithium derivatives which are internally chelated.⁷ Cryoscopic experiments also indicate that an alkenyllithium derivative of stilbene is dimeric in benzene solution.⁸ Hence there is reason to believe that **1** remains associated in solution.

(4) Crystallographic parameters along with a summary of the structure solution can be found in the supplementary material.

(5) The weighting scheme used was the following: $R_w = [\sum(\text{weight} \cdot \nabla^2) / \sum(\text{weight} \cdot F_o^2)]^{1/2}$ where $\nabla = |F_o - F_c|$ and $\text{weight} = 1/[\sigma^2(F_o) + 0.0004F_o^2]$.

(6) The site occupation factors (sof) of the two disordered methylene groups were initially refined as independent variables. However, these values did not differ significantly from 0.5 so they were fixed at this value in the final stages of refinement.

(7) Jastrzebski, J. T. B. J.; van Koten, G.; Konijnen, M.; Stam, C. H. *J. Am. Chem. Soc.* **1982**, *104*, 5490.

(8) Ten Hoedt, R. W. M.; van Koten, G.; Noltes, J. G. *J. Organomet. Chem.* **1979**, *170*, 131.

A short table of important distances and angles for the dimer **2** is given in Figure 2. It is interesting to compare the lithium-lithium distance (2.34 Å) in **2** with the structures of other organolithium derivatives.³ The complex **2** incorporates the shortest lithium-lithium distance yet seen. This distance is significantly shorter than the Li-Li bond in tetrameric methyl lithium (2.57 Å)⁹ or the Li-Li bond in Li₂ (2.67 Å).¹⁰ The lithium atoms in **2** are separated by a distance that approximates that found in hexameric cyclohexyllithium (2.40 Å).¹¹ It is tempting to consider a bonding interaction between the two lithium atoms in **2**. This structure then represents two pentacoordinate lithium atoms surrounded by a distorted trigonal bipyramid and is perhaps the first example of such a pentacoordinate organolithium compound.

We would like to focus on one additional aspect of the dimer **2**. In this associated dimer, the two lithium atoms are located symmetrically above and below (± 0.80 Å) an approximate plane formed by the six nuclei N(1)-C(1)-C(2) and N(1')-C(1')-C(2'). However, the doubly bridging sp² carbon atoms (C(2) and C(2')) are unexceptional and have an analogy in the structures of ferrocenyllithium-PMDT¹² and the tetramer of *o*-LiC₆H₄(CH₂N(CH₃)₂).⁷

The crystal structure of **1** represents the first experimental evidence for an out of plane lithium atom in the structure of a vinyl lithium derivative.

Acknowledgment. R.L.P. and G.S. acknowledge support for this work from the NSF and the NIH. The X-ray crystal structure was recorded at Brown University on an instrument purchased with a grant from the NSF (CHE-8206423).

Supplementary Material Available: Full crystallographic parameters including unit cell parameters, atomic coordinates, thermal parameters, bond lengths and angles, and standard deviations for compound **1** (5 pages). Ordering information is given on any current masthead page.

(9) Weiss, E.; Hencken, G. *J. Organomet. Chem.* **1970**, *21*, 265.

(10) See ref 2, p 67.

(11) Zenger, R.; Rhine, W.; Stucky, G. D. *J. Am. Chem. Soc.* **1974**, *96*, 6048.

(12) Walczak, M.; Walczak, K.; Mink, R.; Rausch, M. D.; Stucky, G. D. *J. Am. Chem. Soc.* **1978**, *100*, 6382.

Near-Infrared Emission in the Catalase-Hydrogen Peroxide System: A Reevaluation

Jeffrey R. Kanofsky

Medical Service, Edward Hines, Jr.
Veterans Administration Hospital
Hines, Illinois 60141

Received March 28, 1984

Chemiluminescence near 1268 nm has recently been demonstrated in a number of peroxidase-H₂O₂-halide systems and evidence has been presented supporting the assignment of this emission to singlet oxygen (¹Δ_g).¹⁻⁵ Khan has reported another near-infrared band at 1640 nm in the catalase-H₂O₂ system, which he attributed to a chemiluminescent process, either an environmentally perturbed singlet oxygen or an energy-transfer process from singlet oxygen to an iron-heme coordination complex.⁴ An alternative hypothesis is that this emission is the result of thermal radiation. The high concentration of H₂O₂ (2.5%) used in Khan's experiments could have resulted in as much as a 17 °C temperature rise during the course of the reaction. Further, this emission

(1) Kanofsky, J. R. *J. Biol. Chem.* **1983**, *258*, 5991.
(2) Khan, A. U.; Gebauer, P.; Hager, L. P. *Proc. Natl. Acad. Sci. U.S.A.* **1983**, *80*, 5195.

(3) Kanofsky, J. R. *J. Biol. Chem.* **1984**, *259*, 5596.

(4) Khan, A. U. *J. Am. Chem. Soc.* **1983**, *105*, 7195.

(5) Kanofsky, J. R.; Tauber, A. I. *Blood* **1983**, *62* (Suppl.), 82a.

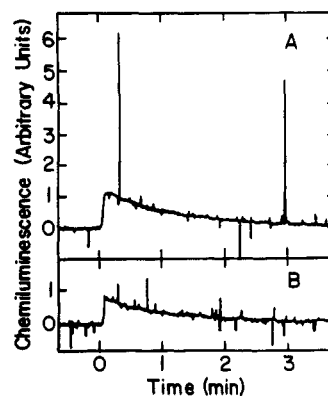


Figure 1. Near-infrared emission of the catalase-H₂O₂ system and of heated H₂O. (A) Injection of 1.5 mL of H₂O₂, 1.5 M, into an equal volume of catalase, 70 μg/mL. Both reactants were in 0.1 M sodium phosphate buffer, pH 7.6. (B) Injection of 1.5 mL of 51 °C H₂O into an equal volume of 24 °C H₂O. Emission was measured through a 1680-nm interference filter. Many noise spikes are seen on each tracing.

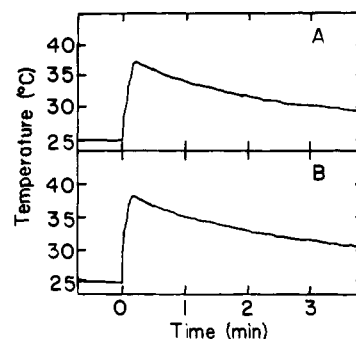


Figure 2. Time course of temperature in the catalase-H₂O₂ system and in heated H₂O. (A) Injection of 1.5 mL of H₂O₂, 1.5 M, into an equal volume of catalase, 70 μg/mL. Both reactants were in 0.1 M sodium phosphate buffer, pH 7.6. (B) Injection of 1.5 mL of 51 °C H₂O into an equal volume of 24 °C H₂O.

Table I. Spectral Distribution of Infrared Emission in the Catalase-H₂O₂ System and in Heated H₂O

nm	filter ^a	
	catalase-H ₂ O ₂ , ^b relative emission ^d	heated H ₂ O, ^c relative emission ^d
1070	-0.01 ± 0.01	0.02 ± 0.02
1170	0.00 ± 0.01	0.00 ± 0.01
1268	0.01 ± 0.01	-0.01 ± 0.01
1370	0.02 ± 0.01	-0.02 ± 0.02
1475	0.06 ± 0.01	0.09 ± 0.01
1580	0.46 ± 0.01	0.41 ± 0.02
1680	1.00 ± 0.02	1.00 ± 0.02
1761	0.47 ± 0.03	0.62 ± 0.03
1880	0.01 ± 0.01	0.03 ± 0.01
1968	0.01 ± 0.01	0.00 ± 0.02

^aSpectral distribution obtained with a set of 10 band-pass interference filters with center frequencies as shown and band widths of 40-50 nm. ^bCatalase, 33 μg/mL; H₂O₂, 0.74 M; 100 mM sodium phosphate buffer, pH 7.6. Emission recorded for 2 min after the initiation of the reaction. ^cEmission from injection of 1.5 mL of 51 °C H₂O into an equal volume of 24 °C H₂O. Emission recorded for 2 min after the injection. ^dNormalized so the peak emission is 1.00 for both systems. Measurements were done in triplicate and reported as the mean ± standard error.

would appear to be an emission band, since the sensitivity of the germanium detector used by Khan decreases rapidly for wavelengths greater than 1600 nm.⁶ Evidence is now presented demonstrating that the near-infrared emission in the catalase-H₂O₂ system is due to thermal radiation.

(6) Data from manufacturer's specifications for Model 403L germanium photodetector (Applied Detector Corp., Fresno, CA) used by Khan.